

miR-451 regulates zebrafish erythroid maturation in vivo via its target *gata2*

Luke Pase,^{1,2} Judith E. Layton,^{1,3} Wigard P. Kloosterman,⁴ Duncan Carradice,^{1,2} Peter M. Waterhouse,⁵ and Graham J. Lieschke¹

¹Walter and Eliza Hall Institute of Medical Research, Parkville, Australia; ²Department of Medical Biology, University of Melbourne, Parkville, Australia;

³Ludwig Institute for Medical Research, The Royal Melbourne Hospital, Parkville, Australia; ⁴Hubrecht Laboratory, Centre for Biomedical Genetics, Utrecht, The Netherlands; and ⁵CSIRO Plant Industry, Canberra, Australia

We demonstrate that in zebrafish, the microRNA miR-451 plays a crucial role in promoting erythroid maturation, in part via its target transcript *gata2*. Zebrafish miR-144 and miR-451 are processed from a single precursor transcript selectively expressed in erythrocytes. In contrast to other hematopoietic mutants, the zebrafish mutant *meunier* (*mnr*) showed intact erythroid specification but diminished miR-144/451 expression. Although erythropoiesis initiated normally in *mnr*, erythrocyte maturation was morphologically retarded. Morpholino knockdown of

miR-451 increased erythrocyte immaturity in wild-type embryos, and miR-451 RNA duplexes partially rescued erythroid maturation in *mnr*, demonstrating a requirement and role for miR-451 in erythrocyte maturation. *mnr* provided a selectively miR-144/451-deficient background, facilitating studies to discern miRNA function and validate candidate targets. Among computer-predicted miR-451 targets potentially mediating these biologic effects, the pro-stem cell transcription factor *gata2* was an attractive candidate. In vivo reporter assays validated the pre-

dicted miR-451/*gata2*-3'UTR interaction, *gata2* down-regulation was delayed in miR-451-knockdown and *mnr* embryos, and *gata2* knockdown partially restored erythroid maturation in *mnr*, collectively confirming *gata2* down-regulation as pivotal for miR-451-driven erythroid maturation. These studies define a new genetic pathway promoting erythroid maturation (*mnr*/miR-451/*gata2*) and provide a rare example of partial rescue of a mutant phenotype solely by miRNA overexpression. (Blood. 2009;113:1794-1804)

Introduction

MicroRNAs (miRNAs) are 19-25 nucleotide, single stranded RNAs that regulate gene expression by binding target mRNAs, modulating their translation and turnover.¹⁻³ However, the biologic role of most individual miRNAs and the targets they modulate remain to be determined.

miRNA expression profiling has been a useful starting point for selecting miRNAs that may influence tissue- or cell-specific processes such as hematopoiesis. High or increasing levels of an miRNA in a specific cell lineage may promote differentiation by repressing transcripts whose persistence or presence would impede cellular commitment (eg, transcripts that promote an alternative cell lineage). On the other hand, high miRNA levels may act to preserve the cellular status quo, as has been proposed in a model of miRNA action in CD34⁺ hematopoietic progenitor cells (HPC).⁴ Conversely, miRNAs of low or falling abundance may be acting to release repression of a set of transcripts necessary to drive changes of cellular state. In view of these various possible mechanisms of action, functional studies are required to understand how individual miRNAs actually influence biologic processes and to determine the molecular mechanisms by which each one acts.

Erythropoiesis is a process of progression from stem cells, characterized by pluripotency and self-renewal, through intermediate states retaining proliferative capacity but of increasingly restricted potential, through to lineage-specific cells that undergo a morphologically recognizable pattern of terminal differentiation. This process requires cells to possess mechanisms for progressive modification of their transcrip-

tones to acquire new capabilities and to discard residual now-redundant or deleterious transcripts from a former cellular state. miRNAs provide a potential mechanism for achieving this.

Several miRNAs are down-regulated as erythropoiesis proceeds, removing constraints that act to preserve a more immature stem or progenitor cellular phenotype. In erythropoietic-driven cultures of human CD34⁺ HPCs, miR-221 and miR-222 are down-regulated.⁵ This contributes to erythroid expansion by derepression of at least one of their targets, *KIT*, through a mechanism verified by HPC transduction with miRNA duplexes or lentiviral overexpression vectors.⁵ Likewise, miR-24 has higher expression in HPCs and is down-regulated during erythroid differentiation.^{4,6} miR-24 represses HPC erythroid differentiation in part through repression of its target, the type I activin receptor (ALK4), thereby gate-keeping the pro-erythropoietic action of activin (in conjunction with erythropoietin) mediated by this receptor.⁶

In contrast, several other miRNAs are strongly up-regulated as erythrocytes mature. Broad expression profiling surveys have recurrently identified miR-144 and miR-451 for their high erythropoietic-restricted expression in several species, including zebrafish,^{7,8} mice,⁹⁻¹¹ and humans.¹¹⁻¹⁵ In mice, they arise from a single transcript.⁹ Overexpression or loss of expression of miR-451 in murine erythroleukemia (MEL) cells promoted or impaired erythrocyte differentiation, respectively, assessed by β -globin transcript abundance and hemoglobinization,¹¹ consistent with miR-451 being a positive regulator of erythroid maturation. A recent

Submitted May 6, 2008; accepted September 16, 2008. Prepublished online as *Blood* First Edition paper, October 10, 2008; DOI 10.1182/blood-2008-05-155812.

The online version of this article contains a data supplement.

The publication costs of this article were defrayed in part by page charge payment. Therefore, and solely to indicate this fact, this article is hereby marked "advertisement" in accordance with 18 USC section 1734.

© 2009 by The American Society of Hematology

study has shown the murine miR-144/451 locus is transcriptionally regulated by Gata1.⁹ Loss of miR-144/451 expression in the zebrafish *gata1*-mutant *vlad tepes* was interpreted as further evidence for Gata1-dependent activation of miR-144/451 locus.⁹ This study also examined loss and gain of miR-451 function in zebrafish embryos, concluding that miR-451 was required for either the maintenance/survival or late-stage maturation of committed erythrocytes.

We independently examined the function of the miR-144/451 in zebrafish hematopoiesis by an alternate experimental approach. We exploited a new zebrafish mutant, *meunier* (*mnr*), a nonanemic mutant expressing *gata1* normally but found to have miR-144/451-deficient erythrocytes. *mnr* freed miR-144/451 from their otherwise epistatic relationship with *gata1* and provided a unique, genetically stable, miR-144/451-deficient but erythrocyte-replete background for experimentation. Using rigorously validated reagents, we demonstrate that miR-451 (but not miR-144) functions to accelerate the kinetics of erythrocyte maturation in zebrafish. Furthermore, we validated *gata2* as one bona fide target of miR-451 in zebrafish, and demonstrate that miR-451-mediated clearance of *gata2* is a crucial influence on the rate of zebrafish erythrocyte maturation.

Methods

Zebrafish

Zebrafish strains used were: AB*, *cloche* (*clo*^{m39}),¹⁶ *Tg(fli1:GFP)*¹,¹⁷ *meunier* (*mnr*^{gl9}, a novel mutant isolated in our ethylnitrosourea mutagenesis screen¹⁸ for its lack of myeloperoxidase [*mpx*] expression) and *Tg(mpx:EGFP)*¹¹⁴.¹⁹ Fish were housed in the Ludwig Institute for Cancer Research Aquarium using standard husbandry practices. All experiments were approved by the Walter and Eliza Hall Institute Animal Ethics Committee. Zebrafish gene, protein, and mutant naming follows the recommended conventions.²⁰

Microinjections

Fertilized 1- to 2-cell embryos were microinjected with 1 to 2 nL synthetic mRNA (50 μg/μL in H₂O), miRNA morpholino oligonucleotides (MOs; 100-500 μmol/L in H₂O; Gene Tools, Philomath, OR), control or *gata2* MOs²¹ (130 μmol/L in H₂O; Gene Tools) and synthetic miRNA duplexes (2-20 μmol/L in H₂O; Sigma-Proligo, St Louis, MO), traced where appropriate by mixing 1:1 with 5% rhodamine dextran (in 0.2 mol/L KCl). We customarily delivered different nucleic acid reagents by separate microinjections to avoid ex vivo mixing. As summarized schematically (Figures 3-6 and Figure S8, available on the *Blood* website; see the Supplemental Materials link at the top of the online article), we selected reagent combinations according to experimental purpose. Some assays required optimization and the specific reagent concentrations used were (1) miRNA duplex/mRNA 3' untranslated region (UTR) validation (Figure S8B,D,E): 50 μg/μL RNA, 2 μmol/L synthetic miRNA duplex; (2) MO validation (Supplementary Figure 8C,F,G): 50 μg/μL RNA, 2 μmol/L synthetic miRNA duplex, 500 μmol/L MO; and (3) miRNA rescue experiments (Figure 3) and *gata2* target validation tests (Figures 4,6), 20 μmol/L synthetic miRNA duplex.

Oligonucleotides and constructs

Table S1 lists oligonucleotide sequences. The green fluorescent protein (GFP) reporter/sensor constructs were derived from pCS2+GFP-F by standard cloning techniques²² and linearized with NotI for in vitro transcription of capped mRNA using the mMACHINE kit (Ambion, Austin, TX). Triplicate miRNA binding sites were constructed by annealing complementary oligonucleotides. The *gata2* miR-451 binding sites were mutated by sequential inverse polymerase chain reaction (PCR) and ligation via an acquired restriction enzyme site. All constructs were validated by sequencing.

Gene expression analysis

Whole mount in situ hybridization (WISH) was performed by using standard techniques and in vitro transcribed digoxigenin- or fluorescein-labeled antisense *gata1*, *gata2*, *hbbe3*, *lcp1*, and *mpx* riboprobes²³⁻²⁶ and 4-nitroblue tetrazolium/5-bromo-4-chloro-3-indolyl phosphate or fast red for detection. miRNA WISH with locked nucleic acid (LNA) probes (Exiqon, Vedbaek, Denmark) was performed as described previously⁸ and with reference to the manufacturer's instructions, using hybridization at 35°C for miR-144, 50°C for miR-451, and 53°C for miR-206 LNA probes. We used standard techniques for double WISH (Figure 2B), probing first with the *hbbe3* riboprobe at 68°C followed by stringent washing and reprobing with the miR-144 LNA probe at 35°C. For adult tissues, dissected organs were diced (1 mm fragments) and processed for WISH as for embryos, with proteinase K (20 μg/mL) treatment for 30 minutes. Organ fragments were aligned in 1% agarose, sectioned, and counterstained with nuclear fast red.

The miR144/451 locus RT-PCR used a Superscript III One-Step reverse transcription (RT)-PCR kit (Invitrogen, Carlsbad, CA) according to the manufacturer's instructions, primers as in Table S1, 30 amplification cycles at 94°C, 60°C, and 68°C for 15, 30, and 30 seconds, respectively, and displaying PCR products by 2% agarose gel electrophoresis.

Imaging

Low-power images were collected using a Nikon SMZ1500 or Nikon 90i fluorescence microscope equipped with a DXM1200c camera and NIS-Elements AR software (Nikon, Tokyo, Japan), and high-power images with a Nikon Optiphot-2 microscope with a Zeiss AxioCam MRc5 digital camera and AxioVision AC (Release 4.5) software (Zeiss, Welwyn Garden City, United Kingdom). Images were imported into Adobe Photoshop CS2 9.0.2 or Illustrator CS2 12.0.1 (Adobe Systems, Mountain View, CA) for orientation and figure preparation. To ensure valid documentation of comparative assessments of fluorescence intensity, arrays of multiple embryos were photographed together in a single image.

Morphometry

Embryonic zebrafish erythrocytes were collected by transecting tails of 6 to 8 embryos in 600 μL of balanced salt solution with 5 mmol/L ethylenediaminetetraacetic acid (EDTA) and 4% fetal calf serum. Cytospin slides were prepared, stained with May-Grünwald/Giemsa stain, and examined at high power. Nuclear and cytoplasmic areas of 20 to 30 randomly selected erythrocytes were measured using either the outline tool of AxioVision AC software or NIS Elements software, and the nuclear/cytoplasmic (N:C) area ratio was calculated. *O*-dianisidine staining for hemoglobin was as described previously.²³

Genotyping

clo embryos were recognized as a Mendelian proportion (Figure 1E). *mnr* embryos were recognized at 48 hours postfertilization (hpf) by their characteristic syndrome of small eyes, cerebral degeneration, and thinner yolk extension. Younger *mnr* embryos were PCR-genotyped at the closely linked (3 centimorgans) simple sequence length polymorphism (SSLP) marker z3984 (oligonucleotides, Table S1; 10 μL reactions; Taq polymerase [New England Biolabs, Ipswich, MA] with supplied buffer; 40 cycles at 95°C, 60°C, and 72°C for 20, 20, and 30 seconds, respectively; PCR products were separated by 2% agarose gel electrophoresis).

Statistics

Single images are representative of at least 30 embryos or representative of *x* of *y* embryos as stated. Quantitative data derives from at least 3 independent experiments; descriptive statistics are either medians or mean plus or minus SD of data for *n* individuals, or mean plus or minus SE of *n* independent experiments. Prism 4.0c (GraphPad Software, San Diego, CA) was used for analytical statistics, using unpaired, 2-tailed *t* tests for normally distributed continuous variables. *P* less than .05 indicated statistically significant difference.

Results

Expression of the zebrafish miR144/451 locus in embryonic and adult erythrocytes

miR-144 and miR-451 form a clustered pair in the genome of zebrafish, separated by only 65 nucleotides (Figure S1). We demonstrated, using RT-PCR, that miR-144 and miR-451 were present on a single transcript (Figure 1A). To determine the anatomical and temporal constraints on their direct function, we examined their expression pattern by whole-mount in situ hybridization. miR-144/451 expression in zebrafish hematopoietic tissues has been previously noted.⁷⁻⁹ The locus was first expressed at 18 hpf in the cytoplasm of individual erythrocytes in the intermediate cell mass (ICM), the axial hematopoietic tissue of the early zebrafish embryo (Figure 1B,C). As expected, embryonic miR-144 expression overlapped with miR-451 expression (Figure 1A,E; data not shown). Early miR-144/451 expression tracked exactly with other genes expressed in erythroid-lineage cells (eg, the erythroid-determining transcription factor *gata1* and globin [*hbbe3*])^{23,26} [Figure 1D,E] and required the presence of erythrocytes. For example, *cloche* (*clo*) is an early hematopoietic/vascular-failure mutant with absent/reduced expression of all known hematopoietic genes.^{16,27,28} miR-144/451 expression was absent in *clo* (Figure 1E), confirming their restricted expression in hemovascular derivatives. The restricted expression of this locus is maintained into adulthood in clusters of cells in the hematopoietic organs (spleen and kidney; Figure 1Fi,ii) and the cytoplasm of circulating erythrocytes (Figure 1Fiii).

meunier, a nonanemic mutant with reduced miR-144/451 expression

The expression of the miR-144/451 locus and other erythroid genes (*gata1*, *hbbe3*) was surveyed in a panel of other hematopoietic-failure mutants. In 8 of 9 mutants from the Melbourne Myeloid screen,¹⁸ there was concordance between miR-144/451 locus and other erythroid gene expression. The single exception was *meunier* (*mnr*), which showed greatly reduced (but not absent) miR-144/451 expression by WISH and semiquantitative RT-PCR despite normal *gata1* and *hbbe3* expression (Figure 2A,B; Figure S2) and normal *O*-dianisidine hemoglobin staining (Figure 2C; Figure S3A).

mnr is an ethylnitrosourea-induced recessive mutant initially identified for its reduced number of myeloperoxidase (*mpx*)-expressing cells (Figure 2D). Expression of myeloid markers that are less lineage-specific (*lcp1*, *lyz*) is reduced, but early hematopoietic transcription factors *tall1* and *spi1* are normal (Figure S4).²⁵ *mnr* develops later nonhematopoietic defects, most significantly cerebral degeneration leading to death at 4 to 5 days postfertilization (dpf). However, until approximately 38 hpf, *mnr* embryos are morphologically indistinguishable from wild-type (WT) siblings (confirmed by longitudinal observation), after which they can be reliably identified by reduced head and eye size (Figure 2C).

The loss of miR-144/451 expression in *mnr* did not merely reflect globally reduced miRNA expression/processing, because expression of the somite-specific miR-206 was normal (Figure 2A),^{8,29} and there was no accumulation of the primary miRNA transcript detected by RT-PCR (Figure S2). Therefore, *mnr* uniquely dissociates miR-144/451 locus expression from its otherwise tight epistatic relationship to *gata1*⁹ without being a global miRNA biogenesis mutant and provides an erythrocyte-replete, genetically stable, miR-144/451-deficient background for further experimentation.

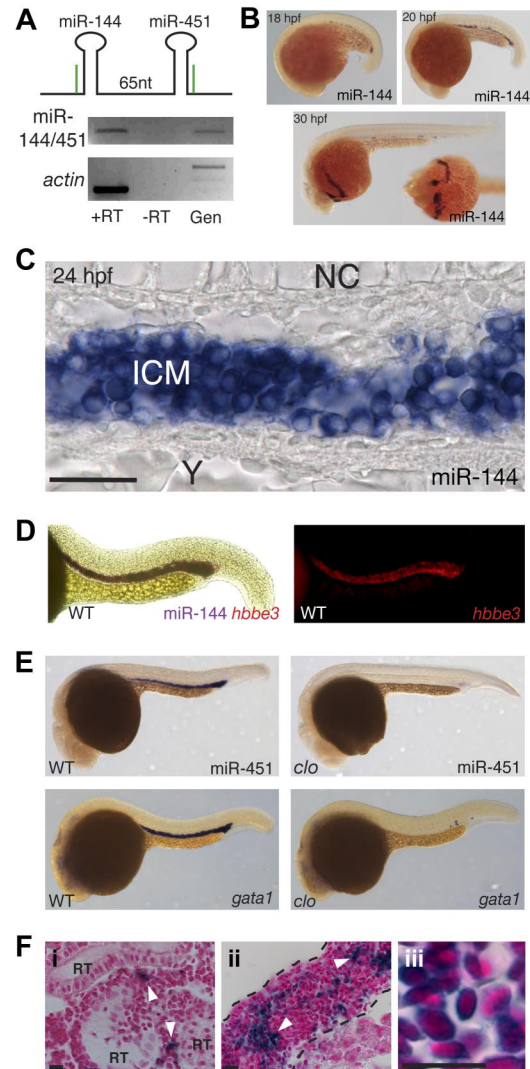


Figure 1. Expression of the miR-144/451 locus in wild-type embryonic and adult zebrafish erythrocytes. (A) miR144/451 locus expression (22 hours postfertilization [hpf]) by RT-PCR using primers confirming that both miRNAs originate from a single precursor transcript. Schema shows primer binding sites in green. RT indicates reverse transcriptase; Gen, genomic DNA control. (B) Whole mount in situ hybridization (WISH) analysis of miR-144 at the 3 embryonic ages shown. miR-144 expression (blue) initiates at 18 hpf in the hematopoietic intermediate cell mass (ICM), becomes confluent across all cells of the ICM (20 hpf), and disperses with erythrocytes at the onset of circulation, pooling over the yolk during fixation for WISH (30 hpf). Lateral views, anterior to left; inset (bottom panel) is ventral view. (C) Sagittal section of 24-hpf WISH embryos showing miR-144 expression (blue) in cytoplasm of erythrocytes of the axial ICM. NC indicates notochord, Y, yolk. Scale bar = 20 μ m. (D) Double WISH showing concordant miR-144 (blue) and *hbbe3* (red) expression. Left panel, bright field; right panel, fluorescence microscopy highlighting *hbbe3* expression. (E) miR-451 and *gata1* expression (blue) in WT and *clo* embryos at 24 hpf, showing concordant loss of *gata1* and miR-451 expression in *clo*. (F) miR-144 expression (blue) in hematopoietic cells nestled between renal tubules (RT) of adult kidney (i, white arrowheads) and the red pulp of the spleen (ii, white arrowheads) in nuclear fast red-counterstained sections cut from tissue fragment in situ hybridization. Detail (iii) shows miR-144 expression localized to the cytoplasm of circulating adult erythrocytes. Scale bar = 10 μ m.

mnr itself is the independent positive regulator of the miR-144/451 locus

Two observations suggest that the miR-144/451-deficiency and *mpx*-deficiency phenotypes of *mnr* are not caused by 2 independent mutations. First, offspring from 3 of 3 independent *mnr* heterozygote pairs genotyped on the basis of their *mpx* deficiency phenotype all showed reduced miR-144/451 expression. Second,

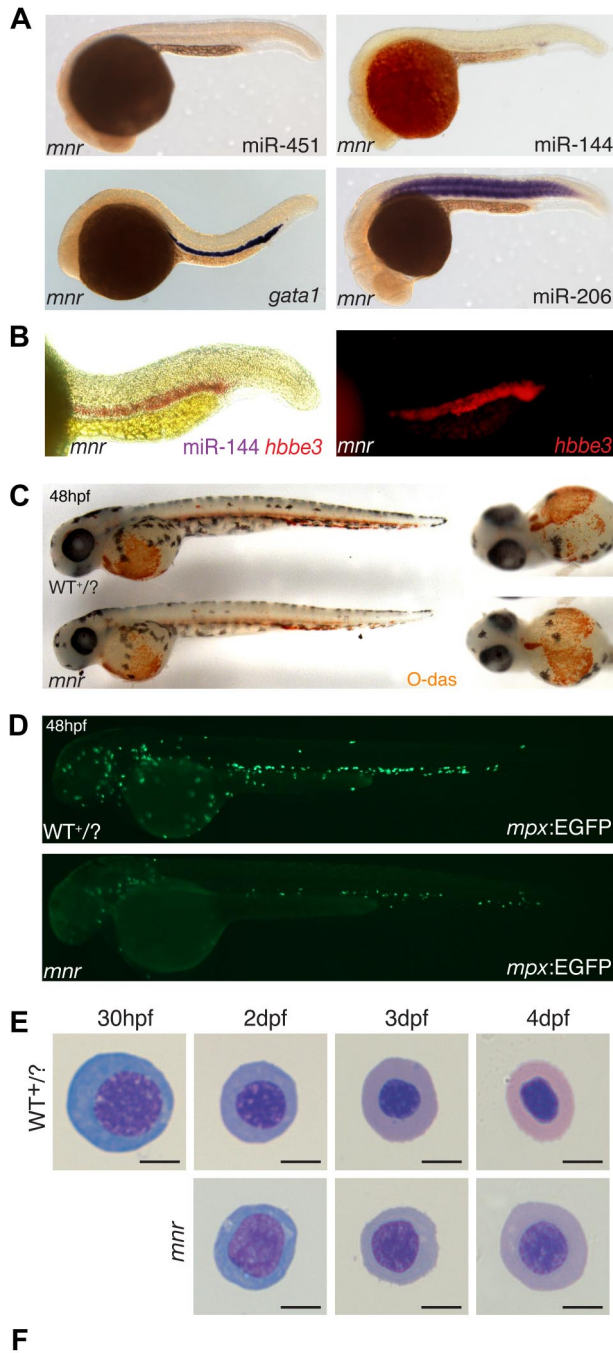


Figure 2. meunier (*mnr*) has miR-144/451 deficiency and an erythroid maturation defect despite normal erythroid specification. (A) Whole-mount in situ hybridization (WISH) expression analysis of miR-144, miR-451, miR-206, and *gata1* at 24 hpf. *mnr* has normal *gata1* expression (compared with wild-type Figure 1E) but is selectively deficient in the 2 erythroid miRNAs. Top panel *mnr* embryos were PCR genotype-confirmed; bottom panel is representative of 57 of 57 (*gata1*) and 32 of 34 (miR-206) embryos resulting from a *mnr* heterozygote incross. (B) Double WISH demonstrating that *mnr* has loss of miR-144 (loss of blue) despite retaining *hbbe3* (red) expression; for comparison with WT, see Figure 1D. Left panel, bright field; right panel, fluorescence microscopy highlighting *hbbe3* expression. (C) Normal expression of hemoglobin (microscopy highlighting *hbbe3* expression). (D) Normal expression of hemoglobin (brown) in *mnr* demonstrated by O-dianisidine (O-das) staining. At 48 hpf, *mnr* is recognizable by its smaller eye and head. Representative embryos are

embryos sorted by either phenotype showed tight linkage to the chromosome 14 SSLP marker z3984 (Figure S5). This tight linkage also means that *mnr* is not a mutation of the miR-144/451 locus itself, because the miR-144/451 locus is on chromosome 5 (Zebrafish Genome Assembly Zv7³⁰).

Erythrocyte maturation is delayed in *mnr*

We hypothesized that *mnr* erythrocytes may exhibit an abnormal phenotype that would point to the nature of their requirement for miR-144/451, and we therefore carefully scrutinized erythroid development in *mnr* mutant embryos. During zebrafish development, there is a characteristic change in erythrocyte morphology associated with developmental age.^{31,32} Proerythroblasts, characterized by deeply basophilic cytoplasm and large finely granular nucleus, mature through stages displaying an increasingly acidic cytoplasm, progressively denser nuclear chromatin, and a decreasing N:C area ratio despite an overall concomitant reduction in erythrocyte diameter (Figure 2E).

Comparing erythrocyte morphology between *mnr* and its WT siblings revealed delayed erythroid maturation in *mnr*. Although evident morphologically (*mnr* erythrocytes were larger, had more basophilic cytoplasm, and more open nuclear chromatin), the N:C ratio (48 hpf) provided a robust objective numeric variable reflecting this delay that was statistically different between *mnr* and WT erythrocytes (Figure 2E,F; Figure S6).

The immaturity of *mnr* erythrocytes was not due to a population skewing effect from loss of mature erythrocytes by apoptosis or from an erythropoietic drive resulting from accelerated erythrocyte destruction, because acridine orange staining failed to demonstrate excess death of ICM hematopoietic cells or later erythroid cells (Figure S7). Overall, *mnr* shows that miR-144/451 are not essential for erythroid specification, early development including hemoglobinization, and survival but suggests their involvement in promoting erythroid maturation.

miR-451 deficiency alone is sufficient to retard erythrocyte maturation

To determine whether miR-144 and/or miR-451 absence alone was sufficient to cause erythrocyte immaturity observed in *mnr*, we used antisense MO knockdown of miR-144 and miR-451.^{9,29} The capability and efficacy of each MO to intercept repressive miRNA/3'UTR interactions was demonstrated by their activity in an in vivo reporter assay based on microinjection of combinations of MO, synthetic miRNA duplexes, and mRNA encoding enhanced green fluorescent protein (EGFP) with a 3'UTR containing canonical

shown in lateral (left) and ventral (right) views to demonstrate equivalent O-das staining despite variation in the pattern of blood pooling at fixation. Embryos are representative of at least 30 embryos/genotype (see also Figure S3A). (D) Deficiency of *mpx*-expressing cells in *mnr*, displayed by a reduced number of EGFP-expressing cells in *mnr* embryos carrying the Tg(*mpx*:EGFP) reporter transgene (bottom panel) compared with wild type (top panel). Figure S4 shows expression of other hematopoietic and myeloid cell markers in *mnr* determined by WISH (*tal1*, *spi1*, *lcp1*, *lyz*, *mpll*). (E) Series of representative circulating erythrocytes from progressively older wild-type (WT + /?, top) and *mnr* (bottom) embryos, demonstrating the progressive maturation of WT erythrocytes and the persistent immature morphology of *mnr* erythrocytes. Erythrocytes are representative of the mean of groups tabulated in panel F. May-Grünwald/Giemsa stain; scale bars = 5 μm. (F) Tabulation of the N:C area ratio in WT and *mnr* embryos from 30 hpf to 4 dpf. The N:C ratio declines in both genotypes but is always greater in *mnr* than in WT. Data are mean plus or minus SD for n embryos, collected over 1 to 4 independent experiments. *P < .001 for WT compared with *mnr*. Figure S6 further demonstrates the reproducibility of these data by presenting them as scatterplots and displaying the interassay variation for the 48-hpf timepoint.

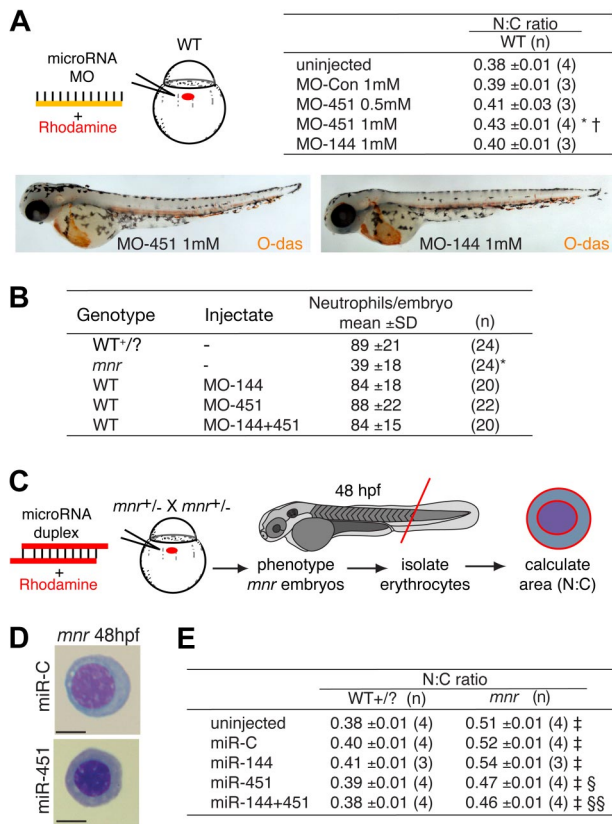


Figure 3. Functional studies of the role of miR-451 in erythroid maturation. (A) miR-451 deficiency, but not miR-144 deficiency, is sufficient to cause erythroid immaturity. MO miRNA antagonists or control MO was microinjected, tracing delivery by rhodamine (schematic diagram) and the N:C area ratio computed as an indicator of maturation (table). O-diansidine staining confirmed normal hemoglobinization in MO-injected embryos at 48 hpf (compare Figure 2C); embryos in panels are representative of at least 16 embryos/group (see Figure S3B). MO reagent validation experiments are in Figure S2. Only MO-451 increased the N:C ratio, reflecting delayed erythrocyte maturation, in a dose-dependent manner. Data are mean plus or minus SE for *n* independent groups from 3 separate experiments. **P* = .036; †*P* = .048 for the comparisons of MO-451-injected with control-injected and MO^{miR-144}-injected groups, respectively, 2-tailed *t* test. Figure S9 further demonstrates the reproducibility of these data by presenting them as scatterplots and providing additional fields of representative cells. (B) Knockdown of miR-144/451 does not affect neutrophil numbers and does not replicate the deficiency of *mpx*-expressing cells in *mnr*. Experiments were performed using WT or *mnr* embryos on the Tg(*mpx:EGFP*) background. Concentration of each MO injected was 1 mmol/L. Neutrophils were quantified by counting EGFP-positive cells/embryo at 48 hpf. **P* < .0001 for comparison of *mnr* with all 4 other groups. (C-E) Overexpression of miR-451, but not miR-144, is sufficient to partially rescue the erythroid maturation block in *mnr*, as evident morphologically (D) and quantitatively (E) using the N:C area ratio. (C) A schema of the experimental design, which required genotyping embryos by nonhematologic phenotypic features at 48 hpf. Data are mean plus or minus SE for *n* independent experiments; ‡*P* < .0025 for line-by-line comparisons of WT to *mnr*, and §*P* = .035 and §§*P* = .003 for the indicated comparisons of miRNA-injected *mnr* with miR-C-injected *mnr*, 2-tailed *t* test. Scale bars = 5 μm. Figure S10 further demonstrates the reproducibility of these data by presenting them as scatterplots and providing additional fields of representative cells.

miRNA target-sites (Figure S8). MO-451 (but not MO-144) resulted in a statistically significant dose-dependent increase in N:C ratio reflecting morphologic erythrocyte immaturity (Figure 3A; Figure S9). However, despite maximal MO doses, this phenotype was not as marked as that observed in *mnr*. MO-451 specifically affected erythrocyte development; MO knockdown of miR144/451 did not affect neutrophil number (Figure 3B), nor did it recapitulate the nonhematologic *mnr* phenotypes. A second MO, MO-451B (of the “multiblocking” type, also interfering with miRNA biogenesis), proved toxic at a dose achieving only modest inhibition in the reporter assay (data not shown). MO-451 affected the rate of erythrocyte maturation but did not abort it, because

O-diansidine staining demonstrated wild-type hemoglobin levels at 48 hpf (Figures 3A, S3B).

miR-451 replenishment partially rescues erythroid maturation in *mnr*

The selective miR-144/451 deficiency of *mnr* provided a scenario for testing whether miRNA replenishment was sufficient to rescue erythrocyte maturation in an endogenously miRNA-deficient environment. Overexpression was achieved by microinjecting a synthetic RNA duplex that mimics the endogenous *dicer* processed product. The activity of synthetic duplexes was confirmed by an *in vivo* reporter assay (Figure S8). Overexpression of miR-451 (but not miR-144) partially rescued the *mnr* erythrocyte maturation defect (Figure 3C-E), reflected morphologically and by a statistically significant reduction in the N:C ratio. This indicates that the *mnr* maturation defect was at least partially due to miR-451 deficiency. In a WT background, overexpression of miR-144/451 did not affect erythrocyte maturation or gross embryo morphology (Figure 3E; Figure S10; data not shown). Furthermore, several nonhematopoietic *mnr* phenotypes were not altered by miR-144/451 overexpression (data not shown), suggesting that they resulted from a role of the *mnr* gene product independent of its role in miR-144/451 up-regulation.

Together, these observations indicate a specific requirement for miR-451 (but not miR-144) in promoting erythroid maturation. The MO-451 knockdown and miR-deficient *mnr* phenotypes indicate a necessity for miR-451 for normal erythrocyte maturation. The partial rescue by miR-451 replenishment in *mnr* indicates that miR-451 is sufficient to promote erythroid maturation in this sensitized genetic background. In all these assays, miR-451 makes a much more critical contribution to erythrocyte maturation than miR-144.

In zebrafish, *gata2* transcripts are a target of miR-451

We used database searching to generate lists of potential mRNA targets of miR-451 that might mediate these biologic effects.³³ miRNA target specificity is conferred by complementary base pairing of its “seed sequence” (nucleotides 2-7) to target mRNAs, and the inhibitory effect is amplified as the number of binding sites in an individual transcript increases.³⁴ As with most miRNAs, miR-451 has numerous potential targets. However, mRNAs encoding transcription factors expressed in the ICM before or during miR-144/miR-451 expression, whose 3'UTR carried 2 or more predicted miRNA binding sites, seemed reasonable candidate targets. Using these criteria, *gata2*, known to preserve the immaturity of hematopoietic precursor cells,³⁵ stood out among 631 predicted targets as an attractive potential target of miR-451 (Figure 4A).

The validity of this prediction was tested using a reporter assay based on monitoring GFP fluorescence in embryos microinjected with mRNA encoding GFP fused to the *gata2*-3'UTR (GFP-3'UTR^{*gata2*}), in the presence or absence of miRNA duplex (Figure 4B-D). In this assay, a decrease in GFP-fluorescence in the presence of duplex indicated miRNA-mediated repression. Embryos sequentially injected with GFP-3'UTR^{*gata2*} reporter and miR-451 showed suppressed GFP-fluorescence, whereas miR-144 had no effect on fluorescence intensity (Figure 4C). This confirmed that the *gata2*-3'UTR was targeted by miR-451 but not by miR-144. The 2 predicted miR-451 binding sites in the *gata2*-3'UTR were validated as bona fide target sequences by further modifications of this assay in which (1) embryos microinjected with mRNA encoding GFP fused to each individual recognition site in triplicate (GFP-3'UTR^{3x} site a

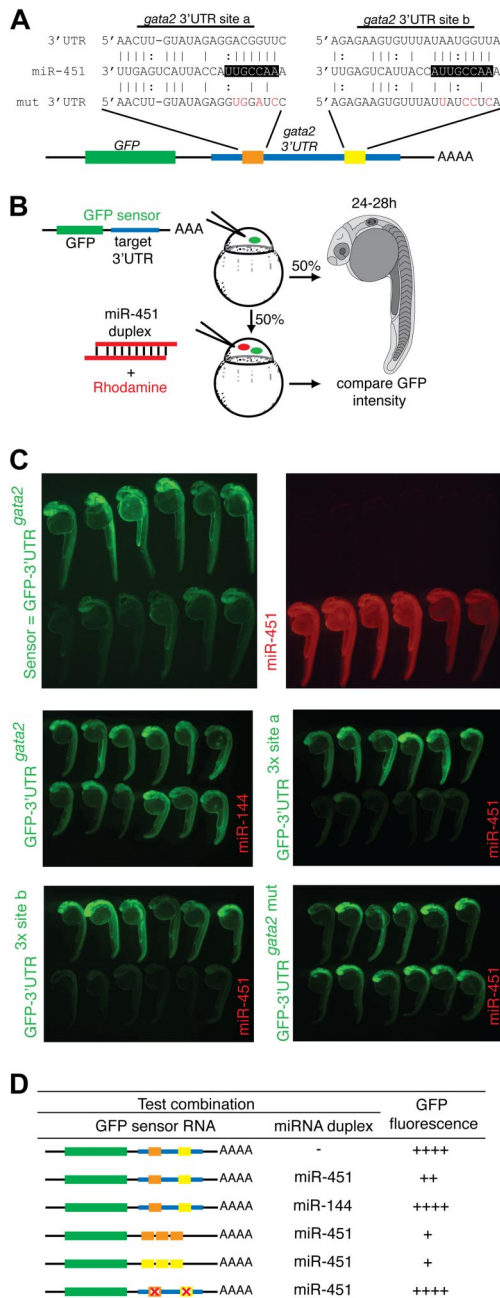


Figure 4. *gata2* is a bona fide target of miR-451. (A) Schematic diagram of the zebrafish *gata2* 3'UTR (blue, nts 128-782), which contains 2 predicted miR-451 binding sites (site a, orange; site b, yellow). Predicted seed complementarity sequences are boxed. Red nucleotides in "mut 3'UTR" indicate those mutated to destroy seed sequence binding. (B) Schema of a reporter assay to evaluate the *gata2*-3'UTR for interaction with miR-451. Microinjection of 1-cell embryos with a series of sensor mRNAs encoding GFP fused to various test 3'UTRs (as tabulated in panel D) was followed by separate injection of 50% of embryos with miR-451 (or mir-144 or control) duplex, tracing miRNA delivery by rhodamine, and the impact on GFP fluorescence intensity assessed at 24 to 28 hpf. (C) miR-451 negatively regulates the sensor GFP-3'UTR^{*gata2*} mRNA. Top: compared with embryos receiving only sensor mRNA (top row in each panel), GFP-fluorescence brightness was reduced in those also injected with miR-451 (traced by rhodamine, red fluorescence in bottom row). Middle and bottom: results of embryos similarly arranged testing various GFP-*gata2*-3'UTR sensor RNA and miRNA combinations as labeled. Arrays of representative embryos were photographed together in a single image to ensure valid comparison of relative green fluorescence intensity between the 2 groups. (D) Summary of reporter assay outcomes using the series of GFP sensor RNA and miRNA combinations, using a comparative scale for GFP fluorescence (+ to +++++). The color-coding of the *gata2*-3'UTR variants in the sensor mRNA column refers to panel A; the red "X" indicates a mutated miR-451 site. Assays validating the bioactivity and specificity of the morpholino and duplex oligonucleotides used are presented in Figure S8.

and GFP-3'UTR^{3x site b}) displayed strong miR-451-induced suppression of GFP-fluorescence (Figure 4C); (2) miR-451-mediated repression on the *gata2*-3'UTR was abolished when both seed sequences were mutated (GFP-3'UTR^{*gata2*-mut}), shown by comparable GFP-fluorescence of this reporter construct alone and in the presence of miR-451 (Figure 4C,D). Collectively, these data prove the capability of miR-451 to target the *gata2*-3'UTR via the 2 predicted recognition sequences.

***gata2* expression is sustained in *mnr* and partly responsible for delayed erythrocyte maturation**

We sought in vivo evidence in support of the hypothesis that miR-451 negatively regulates *gata2*, which predicts an inverse correlation between the presence of *gata2* transcript and miR-451 activity.

First, such an inverse correlation is observed in the wild-type expression dynamics of *gata2* and miR-451. In zebrafish, *gata2* caudal hematopoietic expression initiates in the lateral-plate mesoderm at 10 hpf.^{23,36} These cells give rise to the anterior ICM directly above the yolk extension and the posterior ICM^{37,38} distal to the yolk. After 19 hpf, *gata2* expression decreases substantially in the anterior ICM but is maintained in the posterior ICM.²³ The dynamics of this change in *gata2* expression at 19 hpf coincides with the activation of the miR-144/451 locus in the anterior but not posterior ICM. By 24 hpf, *gata2* expression is nearly completely lost in the strongly miR-451 expressing anterior ICM (comparing miR-451, Figure 1E with *gata2*, Figure 5A).

Second, if miR-451 were involved in the clearance of *gata2* transcripts in the anterior ICM, then in a miR-451-deficient environment such as *mnr* or miR-451 morphant embryos, *gata2* transcripts would persist beyond this transition point. Consistent with this hypothesis, although anterior ICM *gata2* expression is normally nearly completely down-regulated in WT at 24 hpf, in genotyped *mnr* embryos it persisted to 27 hpf and in miR-451 morphants was still present at 24 hpf (Figure 5A). The negative controls (WT siblings, miR-144 morphants, and control-MO-injected embryos) all displayed comparable loss of anterior ICM *gata2* expression at 24 hpf. Up until 48 hpf, erythrocyte *gata2* was not reinstated in *mnr*, miR-451 morphants, WT, or miR-144 morphant controls (data not shown).

Third, we hypothesized that if *mnr* erythroid maturation is delayed because of persistent *gata2* expression, then *gata2* knock-down should rescue the maturation defect of *mnr* (Figure 5B). Strikingly, MO knockdown of *gata2* translation²¹ accelerated erythroid maturation in *mnr* both morphologically and by a significant reduction in N:C ratio (Figure 5C; Figure S11).

Finally, we sought to determine whether *gata2* was the sole miR-451 target responsible for the erythrocyte maturation delay of *mnr*. This was achieved by using the newly described target-blocking MOs,³⁹ which we submitted to a rigorous efficacy and specificity evaluation. MOs complementary to each of the *gata2*-3'UTR miR-451 binding sites (sites a or b as in Figures 4A and 6A; designated MO-TB site a and MO-TB site b) were designed to selectively block endogenous miR-451 binding to the *gata2*-3'UTR, without interfering with the interaction of miR-451 with other target 3'UTRs. The efficacy of these MOs at protecting their respective miR-451 binding site was demonstrated in a set of appropriately designed GFP-fluorescence reporter assays (Figure 6B-D). As a baseline, embryos injected with GFP-3'UTR^{*gata2*} reporter and then miR-451 showed suppressed GFP-fluorescence as previously demonstrated (Figures 4C,6B). In contrast, in the presence of both target blocking MOs (MO-TB-sites a and b), GFP-fluorescence was not suppressed by the presence of miR-451,

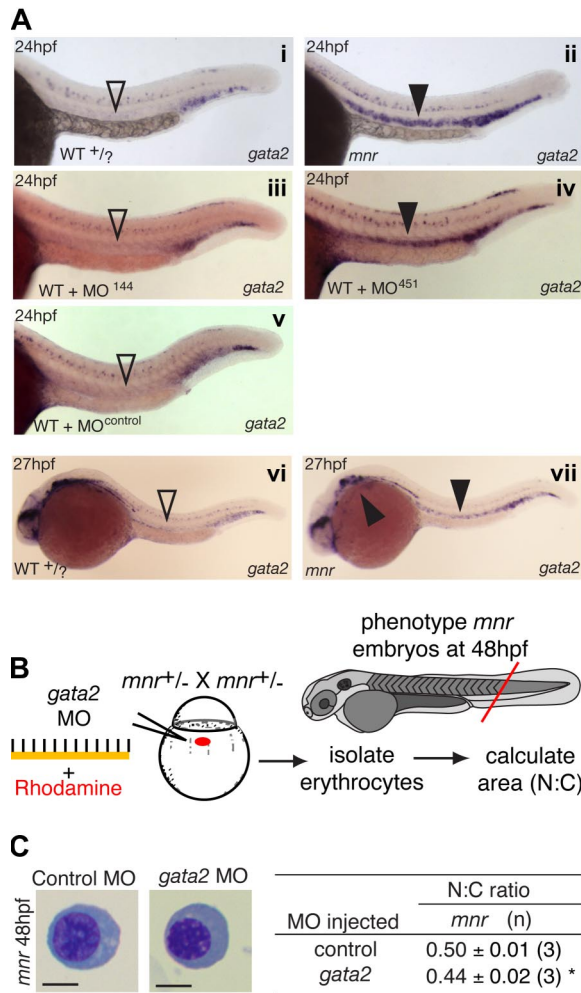


Figure 5. *gata2* and miR-451 interact in vivo to regulate erythrocyte maturation. (A) *gata2* expression (blue) in 24- and 27-hpf embryos by WISH arranged for side-by-side comparison. Left panels (i, iii, v): in wild-type (WT), MO-144- and MO-control-injected embryos, *gata2* expression is waning in the anterior intermediate cell mass at 24 hpf (▽). Right panels (ii, iv); in miR-451-deficient *mnr* and MO-451-injected morphants, *gata2* expression in the anterior intermediate cell mass persists at 24 hpf (▼). (vi, vii) To examine the duration of the persistence of *gata2* expression, a time course of *gata2* expression was examined by WISH at 27-, 30-, 36- and 48-hpf timepoints. At the onset of circulation (27 hpf), sustained *gata2* expression (> WT) was still evident in *mnr* erythrocytes in the anterior intermediate cell mass and over the yolk (vii, solid arrowheads). i and ii are unmanipulated age-matched siblings and representative of 19 of 19 and 11 of 12 PCR-genotype confirmed WT and *mnr* embryos, respectively. Subpanel i, ii, vi, and vii embryos are PCR-genotype confirmed. Subpanels iii through vii are representative of more than 40 age-matched embryos. See Figure 6E legend for further details about controls for comparing the level of *gata2* expression. (B) Schematic diagram of an experiment testing if *gata2* knockdown by a *gata2* MO affects erythrocyte maturation. (C) Results of the experiment in panel B, showing that *gata2* knockdown in *mnr* is sufficient to partially restore erythrocyte maturation (both morphologically and as measured by N:C area ratio). Data are mean plus or minus SE for n independent experiments. **P* = .04, 2-tailed *t* test. Scale bar = 5 μm. Figure S11 further demonstrates the reproducibility of these data by presenting them as scatterplots and providing additional fields of representative cells.

as expected from blocking the miR-451/*gata2*-3'UTR interaction (Figure 6B). This protection was not due simply to the MO-TBs binding to the *gata2*-3'UTR and thereby stabilizing the transcript, because the MO-TB control (designed to bind to the *gata2*-3'UTR between the miR-451 binding sites) did not block the miR-451 suppression of GFP-fluorescence. Further demonstration of the sequence specificity of the MO-TBs and of their inability to bind miR-451 duplexes themselves came from assays in which the GFP-3'UTR^{3x} site a sensor mRNA was protected only by MO-TB

site a but not MO-TB site b, and vice versa (Figure 6C). Together, these evaluations demonstrate that the 2 MO-TBs together block the miR-451/*gata2*-3'UTR interaction in a sequence-specific manner.

Wild-type embryos microinjected with MO-TB sites a and b together showed prolonged *gata2* expression at 24hpf in the anterior ICM (ie, replicating the *mnr gata2* phenotype; Figure 6E), providing evidence both for their functionality in vivo and supporting a direct interaction between endogenous miR-451 and *gata2* in vivo. However, these embryos did not show altered erythrocyte morphology or N:C ratio compared with control embryos (Figure 6F; Figure S12). This suggests that in *mnr* and miR-451 morphant embryos, at least one other miR-451 target needs to be dysregulated to impair erythroid maturation.

Discussion

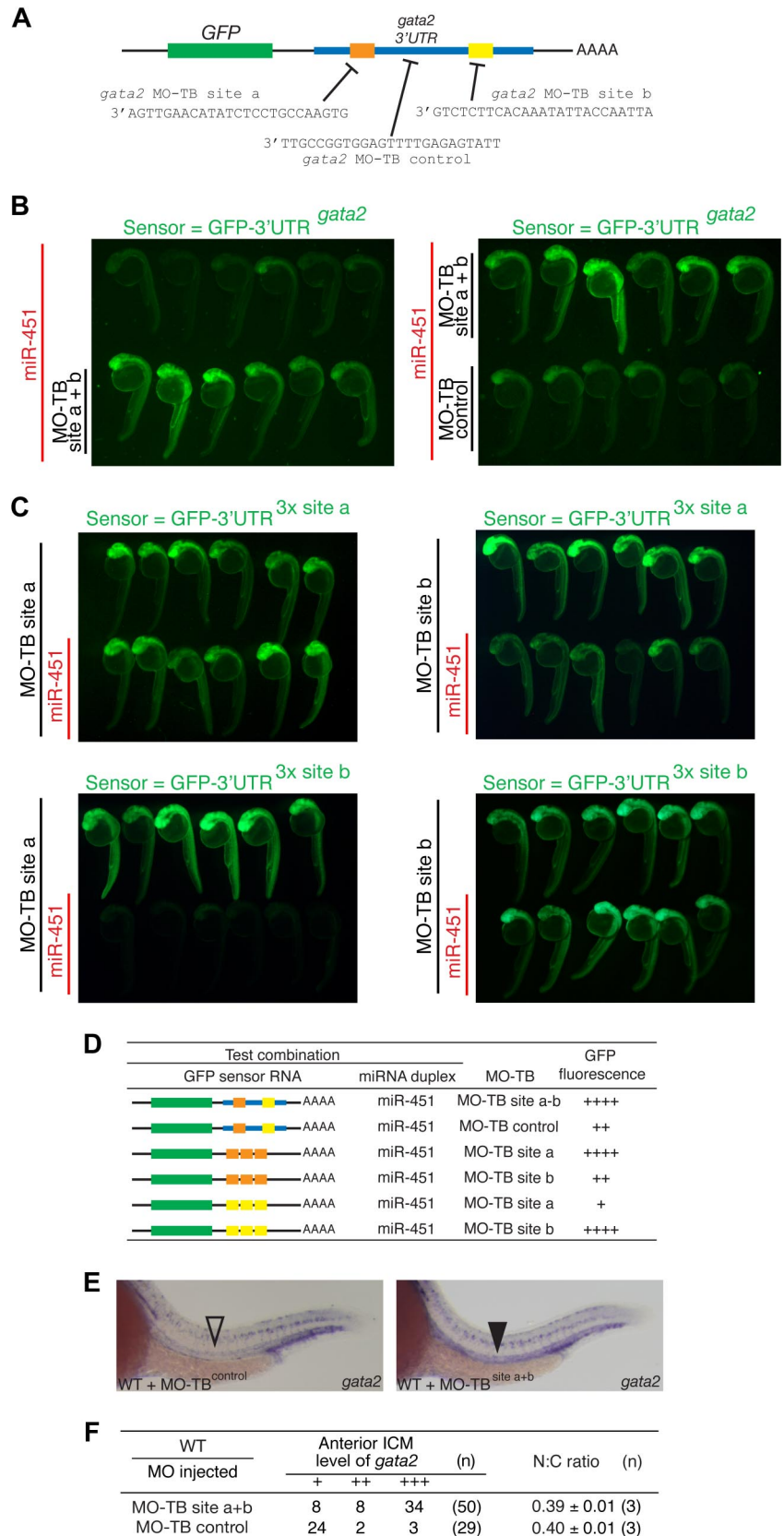
The specific biologic functions of individual miRNAs are now emerging through reverse genetic studies, revealing important roles in development, physiology and disease, including hematopoiesis.^{3,40} Several murine miRNA loci have recently been disrupted by gene targeting with resultant hematopoietic phenotypes (eg, mice lacking miR-155, a lymphoid-restricted miRNA, have defective immune responses^{41,42}; overexpression of miR-155 in murine bone marrow cells drives a myeloproliferative syndrome⁴³; mice lacking miR-223, a granulocyte-lineage-restricted miRNA, have granulocytosis and impaired granulocyte function⁴⁴).

Zebrafish offer several advantages over mice for the study of miRNA function, particularly in developmental processes. In zebrafish, loss- and gain-of-function studies can be undertaken quickly using transient genetic approaches: overexpression by microinjecting a synthetic RNA duplex and miRNA knockdown by injecting an MO antagonist. Predicted miRNA/transcript interactions can be evaluated using fluorescent reporter assays. Interactions between endogenous miRNAs and their targets can be specifically interrupted by target-blocking MOs. Because these approaches are transient, the efficacy and specificity of reagents can be rigorously evaluated quickly and efficiently in vivo in a manner not possible in mice.

However, in wild-type backgrounds, miRNA knockdown/overexpression in zebrafish appears only occasionally to result in any phenotype,^{29,45} and this approach can be technically challenging, particularly to adequately control for spurious effects. A relevant mutant, particularly those that are not epistatic to the pathway of interest, offers advantages such as genetic stability over these transient approaches (eg, the utility of the miRNA biogenesis mutant *dicer* in elucidating the role of miR-430 in early development).^{22,34} However, biogenesis mutants such as this lack numerous miRNAs and have complex later phenotypes^{22,46} that complicate discerning the specific roles of later-expressed miRNAs. A mutant selectively deficient in a particular miRNA but retaining the cell type in which it is expressed would be particularly useful.

We exploited zebrafish reverse genetic techniques to examine the function of the erythroid-restricted miRNAs miR-144 and miR-451, showing that miR-451 accelerated the rate of erythrocyte maturation, an action mediated in part by repression of *gata2*. Our studies were aided by the mutant *mnr*, which dissociated the otherwise invariable link between the presence of erythrocytes and the presence of these 2 miRNAs. *mnr* provided an miR-144/451-deficient model that could independently corroborate observations from other loss-of-function

Figure 6. *gata2* is not the only miR-451 target implicated in regulating erythrocyte maturation (A) Diagram of target blocking (TB) MO designed to protect the 2 *gata2*-3'UTR miR-451 binding sites a and b, and a control MO corresponding to sequences between sites a and b. (B,C) Results of a modification of the reporter assay outlined in Figure 4, for the purpose of validating the efficacy and specificity of the target blocking MOs. For each panel, the sensor RNA was as shown in green. Labels to left of each panel indicate rhodamine-traced miRNA (red labels) and the target blocking MO (MO-TB) delivered to the corresponding rows of embryos. Relative fluorescence intensity between the 2 rows of embryos in each panel assays for miRNA-mediated GFP-sensor-RNA repression. (B) Left panel: a combination of MO-TBs to sites a + b (bottom row of embryos) protect the GFP-*gata2*-3'UTR sensor RNA from miR-451-mediated repression (top row of embryos). Right panel: MO-TB control does not protect against miR-451-mediated repression. (C,D) Panels illustrating other experimental outcomes for different GFP sensor RNA, miRNA and MO-TB combinations as summarized in the Table (D), using a comparative scale for GFP fluorescence (+ to +++++). The color-coding of the *gata2*-3'UTR variants in the sensor mRNA column refers to panel A. (E,F) *gata2* is not the only miR-451 target responsible for the erythrocyte immaturity of *mnr*. *gata2* target-blocking MOs interfere with the *gata2*-3'UTR/miR-451 interaction in vivo, verified by persistence of *gata2* transcripts in the anterior intermediate cell mass (ICM) of 24-hpf embryos (▼ compared with control ▽). Note that there are 3 controls for comparing the level of *gata2* expression: (i) the parallel-processed embryos that received TB-MO-control; (ii,iii) 2 internal controls within each embryo provided by (ii) the comparison of expression in the anterior ICM versus the posterior ICM, and (iii) the comparison between ICM *gata2* expression (which in the anterior ICM is exposed to endogenous miR-451 regulation), and the neuronal *gata2* expression (which is not exposed to endogenous miR-451 expression). (F) Tabulates the anterior ICM level of *gata2* expression by categories (+++, anterior ICM expression as strong as posterior ICM expression; ++, anterior ICM expression less than posterior ICM expression; +, anterior ICM expression absent or less than 30% of posterior ICM expression). n = number of embryos. Despite the effect on *gata2* expression, *gata2* target-blocking MOs did not affect erythrocyte maturation as assessed either morphologically or by the N:C area ratio. N:C ratio data are mean plus or minus SE for n independent experiments. Figure S12 further demonstrates the reproducibility of these data by presenting them as scatterplots and providing additional fields of representative cells.



studies and provided a genetically stable miR-144/451-deficient background “sensitized” for the study of the function of these miRNAs. Indeed, the subtle and somewhat variable effects of miR-451 MO knockdown on erythrocyte maturation were

strongly corroborated by the stronger, more stable, immature erythrocyte phenotype of *mnr*, and the biologic effects of miR-451 overexpression were discernible only on the *mnr* background. *mnr* is not a general miRNA biogenesis mutant, nor

is it a mutation of the miR-144/451 locus itself; exactly how the *mnr* gene product acts as a strong positive regulator of miR144/451 is unknown and will require the identification of the *mnr* mutation.

A recently published study demonstrated that miR-144/451 expression is directly controlled by GATA1, and this was interpreted as GATA1-dependence, based on a comprehensive analysis of the murine locus promoter, and on the loss of miR-144/451 expression in the zebrafish *gata1* mutant *vlad tepes*.⁹ However, *vlad tepes* has markedly defective precirculation ICM erythropoiesis with abundant cell death and is “bloodless” at the onset of circulation^{32,47}; hence, we interpret its loss of miR-144/451 expression to largely reflect the loss of the cells expressing these 2 miRNAs. In contrast, *mnr* expresses ICM *gata1* normally and is erythrocyte-replete but miR-144/451-deficient, thus severing the epistatic relationship between *gata1*-dependent erythrocyte production and miR-144/451 expression. Furthermore, *mnr* indicates that Gata1 requires at least one other gene product, *mnr*, to activate the miR-144/451 promoter. The genetic location of *mnr* on chromosome (Chr) 14 precludes *mnr* from being either *gata1* itself (Chr 11) or several other known or potential components of GATA1-containing transcriptional complexes^{30,48}: *zfpml1/fog1* (Friend-of-gata-1), Chr 18; *klf4* (Krüppel-like factor 4) Chr 2; and *lmo2* (Lim domain only 2) Chr 18.

Our data are consistent with the previous interpretation of miR-451 MO knockdown experiments in zebrafish (ie, that miR-451 is not required for erythroid specification).⁹ However, in contrast to this previous study, we did not observe severe anemia in miR-451 morphant embryos at the onset of circulation or at 48 hpf. The late-onset anemia observed in this other study was interpreted as indicating a requirement for miR-451 in erythrocyte maturation or survival. The reasons for these different outcomes are unclear, particularly because the miR-451 MO sequences were identical, but may reflect subtle differences in MO dose, preparations, or other technical differences. However, our MO knockdown observations are independently corroborated by the erythroid phenotype of *mnr*, which does not show postcirculation erythroid failure, but only delayed erythroid maturation.

Maturation of a population of cells could result either from the progressive maturation of a synchronized cohort of cells, or alternately from the progressive addition of newly produced cells of increasing maturity. Cell survival studies demonstrated that the first cohort of ICM-derived erythrocytes was undiluted by newly produced erythrocytes until 4 dpf³²; hence, we hypothesize that miR-451-dependent promotion of erythrocyte maturation up to 48 hpf is a cell autonomous effect driving the maturation of individual cells.

In mammalian hematopoiesis, persistent production of GATA2 maintains a stem cell phenotype and needs to be down-regulated to allow erythropoiesis to proceed normally.³⁵ One known mechanism for down-regulating GATA2 is by GATA1 directly binding to and repressing its promoter.⁴⁹ An important outcome of our studies was the identification of a mechanism for miR-451 promotion of erythroid maturation in zebrafish: the clearance of *gata2* transcripts. To prove that the prolonged expression of *gata2* in *mnr* and miR-451-morphant erythrocytes was not merely secondary to erythroid immaturity, but directly due to miR-451 loss, we evaluated the *gata2*-3'UTR/miR-451 interaction outside the context of erythrocyte maturation in a direct in vivo reporter assay. This confirmed that a functional interaction occurred. We also evaluated the cause/effect biologic consequences of perturbing this interaction: rerepressing *gata2* in miR-451-deficient *mnr* with

MO-*gata2* and relieving *gata2* alone of miR-repression in WT with the target-blocking MOs.

Repression of *GATA2* by this miRNA locus may be conserved in mammals, although it may be achieved through miR-144 rather than miR-451, because human, murine, and rat *GATA2*-3'UTRs all contain several predicted miR-144 binding sites but no predicted miR-451 sites (Table S2). The in vivo GFP reporter assay provides a method for evaluating the functional validity of these potential miRNA/transcript interactions.

Gata1 displaces Gata2 from the murine miR-144/451 promoter to activate promoter function.⁹ Hence, in zebrafish, at least, there is scope for a 2-pronged Gata1-driven regulatory mechanism for relaxing Gata2 repression of erythroid maturation; Gata1 turns off further *gata2* transcription and activates transcription of a miRNA locus that down-regulates extant *gata2* transcripts.

We interpret the failure of MOs exclusively interfering with the miR-451/*gata2* interaction to repress erythrocyte maturation to indicate that miR-451 targets other than *gata2* are also important in erythrocyte maturation. This indicates that there is redundancy and robustness in miR-451-driven erythroid maturation. Reporter assays and *mnr*-based functional assays provide a

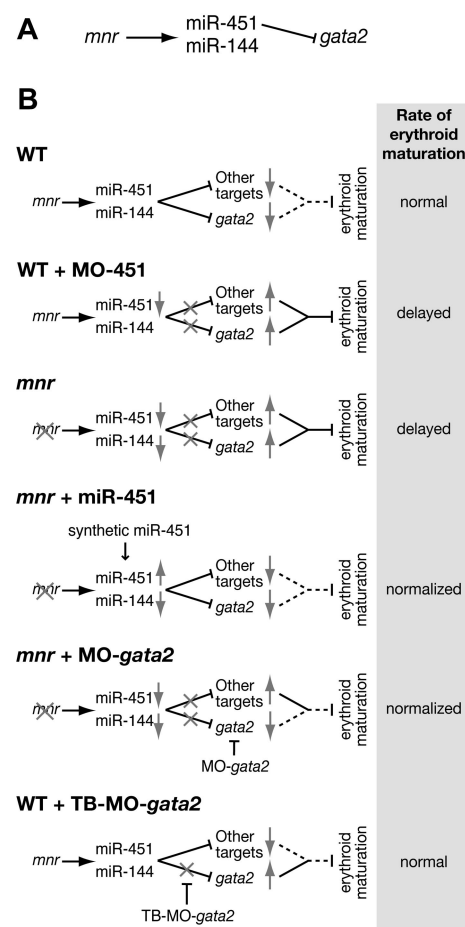


Figure 7. miR-144 and miR-451 in zebrafish erythroid development. (A) Genetic pathway connecting the mutation *meunier* (*mnr*), the microRNAs miR-144 and miR-451, and the miR-451 target *gata2*. (B) Models of the biologic impact of this genetic pathway on erythroid maturation, in wild-type, and in various perturbed scenarios. Gray arrows indicate reduced (↓) or increased (↑) net level of activity at steps of the genetic pathway. Gray crosses (X) indicate the level of block in the pathway in the individual scenarios. For the net biologic outcome of the genetic pathway on repression of erythroid maturation, a dotted line indicates a normal (ie, wild-type) level of repression, and a continuous line indicates a stronger-than-normal repressive effect. TB-MO indicates target-blocking morpholino oligonucleotide.

basis for evaluating other candidate target transcripts carrying putative miR-451 binding sites for their role in erythrocyte maturation. An alternate hypothesis is that the target blocking MOs alter the dose of *Gata2* but not as much as in *mnr* or miR-451 morphants.

Together, our results assemble a new genetic pathway that regulates the pace of erythroid maturation: *mnr* activating miR-451, which in turn represses *gata2* (Figure 7A). This genetic pathway informs a biologic model (Figure 7B) consistent with our experimental observations. In general, once committed to an erythroid fate, cells require *mnr* to use miR-451 to down-regulate repressors of erythroid maturation, *gata2* being one of them. miR-451 deficiency (either MO-451 morphants or *mnr* mutants) retards the pace of erythroid maturation by permitting *gata2* and other target transcripts to persist longer than usual. In *mnr*, normalizing levels either of miR-451 alone or of its target *gata2* (by restoring miR-451 levels or by *gata2* knockdown) is sufficient to partially rescue the rate of red cell maturation. However, because *gata2* target-blocking MOs are insufficient to retard erythrocyte maturation in wild-type embryos, there must be other miR-451 targets that need to be codysregulated to result in the erythrocyte immaturity of *mnr* or miR-451 morphants. Finally, these experiments exemplify an hypothesized miRNA role in sharpening developmental transitions,^{34,50} in this case from a hematopoietic progenitor cell into a maturing erythrocyte.

Acknowledgments

We thank the following for helpful discussions, encouragement, support, and/or technical help: Warren Alexander, Tony Burgess, Stephen Cody, David Curtis, John Hayman, Joan Heath, Ben

Hogan, Stephen Jane, Luke Kapitany, Anne Lagendijk, Nick Nicola, Sony Varma, and colleagues in the Colon Molecular and Cell Biology Group at the Ludwig Institute and the Bone Marrow Research Laboratory (Royal Melbourne Hospital). We particularly thank Belinda Phipson and Gordon Smyth for statistical advice and Stephen Renshaw for supplying the Tg(*mpx*:EGFP) line. We thank several anonymous reviewers for constructive criticism and suggestions that improved the manuscript.

This work was supported in part by grants from the National Institutes of Health (Bethesda, MD; R01-HL079545) and National Health and Medical Research Council (NHMRC 461222 and 461208) to G.L. L.P. was supported by an Australian Postgraduate Award and CSIRO enhancement stipend and received travel support from the ARC/NHMRC Network in Genes and Environment in Development (NGED).

Authorship

Contribution: L.P. designed, conducted, and interpreted the experiments and wrote the manuscript; J.E.L. generated the mutant *meunier* and initiated its mapping; W.P.K. performed miR-451 and miR-206 in situ hybridizations; D.C. performed some in situ hybridizations and made early contributions to *mnr* mapping and erythrocyte morphometrics; P.M.W. helped plan the studies and cosupervised L.P.; and G.J.L. designed and interpreted the experiments, supervised L.P., and wrote the manuscript.

Conflict-of-interest disclosure: The authors declare no competing financial interests.

Correspondence: Dr Graham J. Lieschke, Walter and Eliza Hall Institute of Medical Research, 1G Royal Parade, Parkville, VIC, Australia 3050; e-mail: lieschke@wehi.edu.au.

References

- Bartel DP. MicroRNAs: genomics, biogenesis, mechanism, and function. *Cell*. 2004;116:281-297.
- Pillai RS, Bhattacharyya SN, Filipowicz W. Repression of protein synthesis by miRNAs: how many mechanisms? *Trends Cell Biol*. 2007;17:118-126.
- Stefani G, Slack FJ. Small noncoding RNAs in animal development. *Nat Rev Mol Cell Biol*. 2008;9:219-230.
- Georgantas RW, 3rd Hildreth R, Morisot S, et al. CD34+ hematopoietic stem-progenitor cell microRNA expression and function: a circuit diagram of differentiation control. *Proc Natl Acad Sci U S A*. 2007;104:2750-2755.
- Felli N, Fontana L, Pelosi E, et al. MicroRNAs 221 and 222 inhibit normal erythropoiesis and erythroleukemic cell growth via kit receptor down-modulation. *Proc Natl Acad Sci U S A*. 2005;102:18081-18086.
- Wang Q, Huang Z, Xue H, et al. MicroRNA miR-24 inhibits erythropoiesis by targeting activin type I receptor ALK4. *Blood*. 2008;111:588-595.
- Kloosterman WP, Steiner FA, Berezikov E, et al. Cloning and expression of new microRNAs from zebrafish. *Nucleic Acids Res*. 2006;34:2558-2569.
- Wienholds E, Kloosterman WP, Miska E, et al. MicroRNA expression in zebrafish embryonic development. *Science*. 2005;309:310-311.
- Dore LC, Amigo JD, Dos Santos CO, et al. A GATA-1-regulated microRNA locus essential for erythropoiesis. *Proc Natl Acad Sci U S A*. 2008;105:3333-3338.
- Monticelli S, Ansel KM, Xiao C, et al. MicroRNA profiling of the murine hematopoietic system. *Genome Biol*. 2005;6:R71.
- Zhan M, Miller CP, Papayannopoulou T, Stamatoyannopoulos G, Song CZ. MicroRNA expression dynamics during murine and human erythroid differentiation. *Exp Hematol*. 2007;35:1015-1025.
- Bruchova H, Yoon D, Agarwal AM, Mendell J, Prchal JT. Regulated expression of microRNAs in normal and polycythemia vera erythropoiesis. *Exp Hematol*. 2007;35:1657-1667.
- Landgraf P, Rusu M, Sheridan R, et al. A mammalian microRNA expression atlas based on small RNA library sequencing. *Cell*. 2007;129:1401-1414.
- Masaki S, Ohtsuka R, Abe Y, Muta K, Umemura T. Expression patterns of microRNAs 155 and 451 during normal human erythropoiesis. *Biochem Biophys Res Commun*. 2007;364:509-514.
- Rathjen T, Nicol C, McConkey G, Dalmay T. Analysis of short RNAs in the malaria parasite and its red blood cell host. *FEBS Lett*. 2006;580:5185-5188.
- Stainier DY, Weinstein BM, Detrich HW III, Zon LI, Fishman MC. Cloche, an early acting zebrafish gene, is required by both the endothelial and hematopoietic lineages. *Development*. 1995;121:3141-3150.
- Lawson ND, Weinstein BM. In vivo imaging of embryonic vascular development using transgenic zebrafish. *Dev Biol*. 2002;248:307-318.
- Hogan BM, Layton JE, Pyati UJ, et al. Specification of the primitive myeloid precursor pool requires signaling through Alk8 in zebrafish. *Curr Biol*. 2006;16:506-511.
- Renshaw SA, Loynes CA, Trushell DM, Elworthy S, Ingham PW, Whyte MK. A transgenic zebrafish model of neutrophilic inflammation. *Blood*. 2006;108:3976-3978.
- Zebrafish Nomenclature Committee. Zebrafish nomenclature guidelines. http://zfinfo.org/zf_info/nomen.html#2. Accessed April 23, 2008.
- Galloway JL, Wingert RA, Thisse C, Thisse B, Zon LI. Loss of *gata1* but not *gata2* converts erythropoiesis to myelopoiesis in zebrafish embryos. *Dev Cell*. 2005;8:109-116.
- Giraldez AJ, Cinalli RM, Glasner ME, et al. MicroRNAs regulate brain morphogenesis in zebrafish. *Science*. 2005;308:833-838.
- Detrich HW, Kieran MW 3rd, Chan FY, et al. Intraembryonic hematopoietic cell migration during vertebrate development. *Proc Natl Acad Sci U S A*. 1995;92:10713-10717.
- Herbomel P, Thisse B, Thisse C. Ontogeny and behaviour of early macrophages in the zebrafish embryo. *Development*. 1999;126:3735-3745.
- Lieschke GJ, Oates AC, Crowhurst MO, Ward AC, Layton JE. Morphologic and functional characterization of granulocytes and macrophages in embryonic and adult zebrafish. *Blood*. 2001;98:3087-3096.
- Brownlie A, Hersey C, Oates AC, et al. Characterization of embryonic globin genes of the zebrafish. *Dev Biol*. 2003;255:48-61.
- Thompson MA, Ransom DG, Pratt SJ, et al. The cloche and spadetail genes differentially affect hematopoiesis and vasculogenesis. *Dev Biol*. 1998;197:248-269.

28. Liao EC, Paw BH, Oates AC, Pratt SJ, Postlethwait JH, Zon LI. SCL/Tal-1 transcription factor acts downstream of cloche to specify hematopoietic and vascular progenitors in zebrafish. *Genes Dev.* 1998;12:621-626.
29. Kloosterman WP, Legendijk AK, Ketting RF, Moulton JD, Plasterk RH. Targeted inhibition of miRNA maturation with morpholinos reveals a role for miR-375 in pancreatic islet development. *PLoS Biol.* 2007;5:e203.
30. Zebrafish (*Danio rerio*) sequencing project. http://www.sanger.ac.uk/Projects/D_rerio/wgs.shtml. Accessed April 16, 2008.
31. Qian F, Zhen F, Xu J, Huang M, Li W, Wen Z. Distinct functions for different scl isoforms in zebrafish primitive and definitive hematopoiesis. *PLoS Biol.* 2007;5:e132.
32. Weinstein BM, Schier AF, Abdelilah S, et al. Hematopoietic mutations in the zebrafish. *Development.* 1996;123:303-309.
33. Griffiths-Jones S, Grocock RJ, van Dongen S, Bateman A, Enright AJ. miRBase: microRNA sequences, targets and gene nomenclature. *Nucleic Acids Res.* 2006;34:D140-144.
34. Giraldez AJ, Mishima Y, Rihel J, et al. Zebrafish MiR-430 promotes deadenylation and clearance of maternal mRNAs. *Science.* 2006;312:75-79.
35. Minegishi N, Suzuki N, Yokomizo T, et al. Expression and domain-specific function of GATA-2 during differentiation of the hematopoietic precursor cells in midgestation mouse embryos. *Blood.* 2003;102:896-905.
36. Patterson LJ, Gering M, Eckfeldt CE, et al. The transcription factors Scl and Lmo2 act together during development of the hemangioblast in zebrafish. *Blood.* 2007;109:2389-2398.
37. Bertrand JY, Kim AD, Violette EP, Stachura DL, Cisson JL, Traver D. Definitive hematopoiesis initiates through a committed erythromyeloid progenitor in the zebrafish embryo. *Development.* 2007;134:4147-4156.
38. Kissa K, Murayama E, Zapata A, et al. Live imaging of emerging hematopoietic stem cells and early thymus colonization. *Blood.* 2008;111:1147-1156.
39. Choi WY, Giraldez AJ, Schier AF. Target protectors reveal dampening and balancing of Nodal agonist and antagonist by miR-430. *Science.* 2007;318:271-274.
40. Kloosterman WP, Plasterk RH. The diverse functions of microRNAs in animal development and disease. *Dev Cell.* 2006;11:441-450.
41. Rodriguez A, Vigorito E, Clare S, et al. Requirement of bic/microRNA-155 for normal immune function. *Science.* 2007;316:608-611.
42. Thai TH, Calado DP, Casola S, et al. Regulation of the germinal center response by microRNA-155. *Science.* 2007;316:604-608.
43. O'Connell RM, Rao DS, Chaudhuri AA, et al. Sustained expression of microRNA-155 in hematopoietic stem cells causes a myeloproliferative disorder. *J Exp Med.* 2008;205:585-594.
44. Johnnidis JB, Harris MH, Wheeler RT, et al. Regulation of progenitor cell proliferation and granulocyte function by microRNA-223. *Nature.* 2008;451:1125-1129.
45. Cao X, Pfaff SL, Gage FH. A functional study of miR-124 in the developing neural tube. *Genes Dev.* 2007;21:531-536.
46. Wienholds E, Koudijs MJ, van Eeden FJ, Cuppen E, Plasterk RH. The microRNA-producing enzyme Dicer1 is essential for zebrafish development. *Nat Genet.* 2003;35:217-218.
47. Lyons SE, Lawson ND, Lei L, Bennett PE, Weinstein BM, Liu PP. A nonsense mutation in zebrafish *gata1* causes the bloodless phenotype in *vlad tepes*. *Proc Natl Acad Sci U S A.* 2002;99:5454-5459.
48. Ferreira R, Ohneda K, Yamamoto M, Philipsen S. GATA1 function, a paradigm for transcription factors in hematopoiesis. *Mol Cell Biol.* 2005;25:1215-1227.
49. Grass JA, Boyer ME, Pal S, Wu J, Weiss MJ, Bresnick EH. GATA-1-dependent transcriptional repression of GATA-2 via disruption of positive autoregulation and domain-wide chromatin remodeling. *Proc Natl Acad Sci U S A.* 2003;100:8811-8816.
50. Schier AF, Giraldez AJ. MicroRNA function and mechanism: insights from zebra fish. *Cold Spring Harb Symp Quant Biol.* 2006;71:195-203.